arXiv:2208.02268v2 [quant-ph] 17 Nov 2023

Anomalous criticality with bounded fluctuations and long-range frustration induced by broken time-reversal symmetry

Jinchen Zhao[1] and Myung-Joong Hwang[1,2,*]

[1]*Division of Natural and Applied Sciences, Duke Kunshan University, Kunshan, Jiangsu, 215300 China*
[2]*Zu Chongzhi Center for Mathematics and Computational Science, Duke Kunshan University, Kunshan, Jiangsu, 215300 China*

We consider a one-dimensional Dicke lattice with complex photon hopping amplitudes and investigate the influence of time-reversal symmetry breaking due to synthetic magnetic fields. We show that, by tuning the total flux threading the lattice with a periodic boundary condition, the universality class of superradiant phase transition (SPT) changes from that of the mean-field fully-connected systems to one that features anomalous critical phenomena. The anomalous SPT exhibits a closing of the energy gap with different critical exponents on both sides of transition and a discontinuity of correlations and fluctuation despite it being a second-order phase transition. In the anomalous normal phase, we find that a non-mean-field critical exponent for the closing energy gap and non-divergent fluctuations and correlations appear, which we attribute to the asymmetric dispersion relation. Moreover, we show that the nearest neighborhood complex hopping induces effective long-range interactions for position quadratures of the cavity fields, whose competition leads to a series of first-order phase transitions among superradiant phases with varying degrees of frustration. The resulting multicritical points also show anomalous features such as two coexisting critical scalings on both sides of the transition. Our work shows that the interplay between the broken time-reversal symmetry and frustration on bosonic lattice systems can give rise to anomalous critical phenomena that have no counter-part in fermionic, spin or time-reversal symmetric quantum optical systems.

Introduction.— Inspired by the discovery of remarkable phenomena for charged particles moving in magnetic fields such as integer and fractional quantum Hall effects [1, 2], there have been intense theoretical and experimental efforts to realize synthetic magnetic fields for uncharged particles such as photons [3–7], phonons [8, 9] and neutral atoms [10, 11]. In a lattice of photonic resonators, for example, the synthetic magnetic fields have been realized to observe unique topological photonic properties and robust edge states [12–14]. Moreover, the chiral photon current due to the time-reversal symmetry breaking induced by synthetic magnetic fields has also been observed [5]. The light-matter interaction between such chiral photons and quantum emitters may give rise to novel quantum optical phenomena [15–19].

A bosonic mode coupled to two-level systems, described by the Dicke model, exhibits a superradiant phase transition (SPT) [20–27] when the spin-boson coupling strength exceeds a threshold. The SPT of the Dicke model belongs to the universality class of fully-connected systems characterized by the mean-field exponents [23, 28–31]; thus, we refer to it as mean-field SPT. Finding SPTs that exhibit critical phenomena that don't belong to this universality class may lead to a discovery of novel phases of coupled light and matter; recently discovered examples include spin glass phases induced by the multimode cavity fields [32–39] and a frustrated SPT in the Dicke lattice [40]. Also, a tricritical SPT in the Rabi lattice in the synthetic magnetic field has been discovered [41, 42].

In this Letter, we investigate a one-dimensional Dicke lattice model with complex photon hopping amplitudes, whose phase determines the magnetic flux threading the lattice under periodic boundary conditions. We discover that there exists a multicritical magnetic flux point θ_c, above which a mean-field SPT occurs [27, 31, 43] and below which an *anomalous* SPT occurs with unusual critical properties that do not belong to the universality class of the fully-connected systems. The anomalous SPT features an anomalous normal phase (NP) in which the fluctuation and correlation do not diverge at the critical point, which shatters the common belief that they always diverge at the critical point. Moreover, the critical exponent of the closing energy gap abruptly changes from a mean-field exponent $1/2$ above θ_c (NP) to 1 below θ_c (anomalous NP); at θ_c, both critical exponents coexist. We show that the anomalous NP emerges when the critical mode acquires a finite momentum, which has an asymmetric dispersion relation due to the time-reversal symmetry breaking. The broken symmetry phase of the anomalous SPT, on the other hand, exhibits a diverging correlation with the critical exponent that are different from that of anomalous NP. Furthermore, we construct an effective semiclassical model for the position quadratures with long-range effective photon hopping interactions. Our effective theory shows that the first-order phase transition from the mean-field to the anomalous superradiant phase occurs when the position quadrature of cavity coherences exhibits frustration. The configuration of order parameters is determined by the relative signs of the effective nearest and the next-nearest interaction, analogous to the J_1-J_2 Ising model, and therefore a series of first-order phase transitions and multicritical points may emerge as the magnetic flux modulates the sign of both interactions.

Our study therefore shows that the presence of the synthetic magnetic field gives rise to the anomalous SPT and anomalous multicritical points with critical properties that has no counterpart in time-reversal symmetric case [40] and that are not commonly found in statistical physics systems [44–46]; two most important characteristics of the anomalous SPT are the following: 1) critical exponents on both sides of the critical point

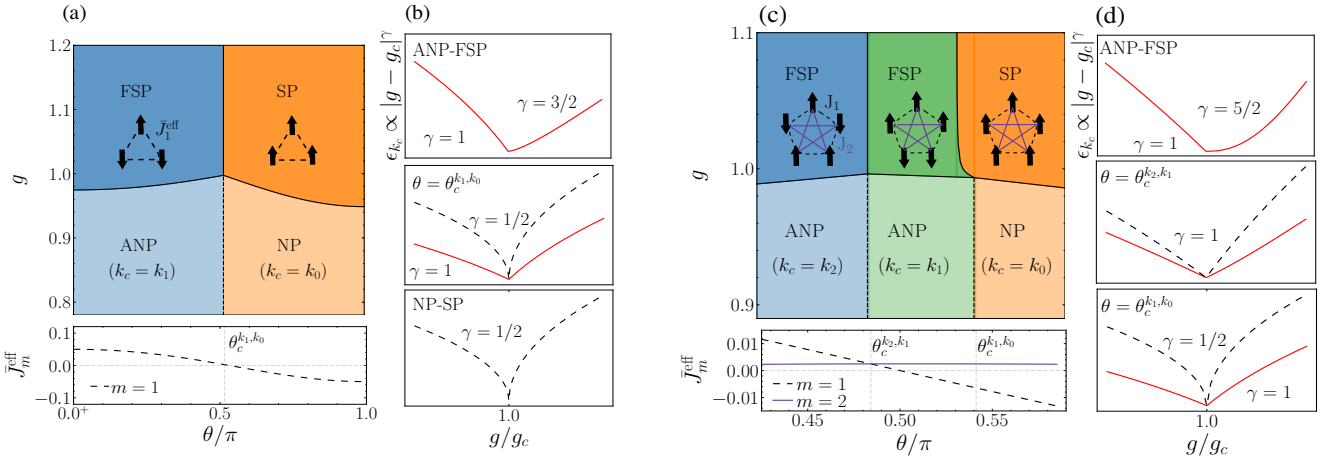


FIG. 1. Phase diagrams and excitation energies for (a)(b) $N = 3$ and (c)(d) $N = 5$. (a) and (c) Top panel: Phase diagram in the $g - \theta$ space. Here, NP and SP represent the normal and superradiant phase, respectively, while ANP and FSP stand for anomalous NP and frustrated SP, respectively. k_c is the momentum of the critical mode in NP, and $k_j = -2\pi j/N$. The arrows denote the sign configurations of the mean values $x_n = \mathrm{Re}(\langle a_n \rangle)$, where up arrows denote $x_n > 0$, and down arrows denote $x_n < 0$. The lines connecting lattice sites correspond to the effective hopping shown in the bottom panel. (a) and (c) Bottom panel: The effective photon hopping $\bar{J}_m^{\rm eff}$ in the mean-field energy as a function of θ. Here, $\bar{J}_1^{\rm eff}$ is the nearest-neighbor hopping, while $\bar{J}_2^{\rm eff}$ is the next-nearest-neighbor hopping. (b) and (d) Critical excitation energies as a function of g for different values of θ. Here, γ denotes the scaling of the corresponding excitation, and the upper-right labels denote the region the SPT belongs to. ANP-FSP corresponds to $0 < \theta < \theta_c^{k_1,k_0}$, except for the flux critical points $\theta_c^{k_{j+1},k_j}$ (note that the time-reversal symmetric case [40] is excluded). NP-SP corresponds to $\theta_c^{k_1,k_0} < \theta < \pi$.

are different from each other; this adds an experimentally accessible counter-example to the common expectation that critical exponents on both sides of the critical point are same due to the identical renormalization group properties [47]. 2) The fluctuation and correlation are *bounded* at the critical point in the anomalous NP and therefore they become discontinuous across the anomalous SPT, despite it being a second-order phase transition.

Model.— We consider a Dicke lattice model where each lattice site realizes the Dicke model and neighboring lattices are connected by the photon hopping interaction with complex amplitudes. The model Hamiltonian reads

$$H_N = \sum_{n=1}^{N} \left[H_n + J \left(e^{i\theta} a_n^\dagger a_{n+1} + h.c. \right) \right]$$
$$H_n = \omega a_n^\dagger a_n + \Omega J_n^z + \frac{2\lambda}{\sqrt{N_a}} \left(a_n + a_n^\dagger \right) J_n^x \tag{1}$$

with a periodic boundary condition $a_{N+1} = a_1$ to form a loop. The phase $\theta \in (0, \pi)$ represents the total flux of synthetic magnetic fields threading the loop. At nth lattice site, the oscillator of frequency ω is described by an annihilation operator a_n and there is an ensemble of N_a spins of frequency Ω described by collective spin operators $J_n^{x,z}$. λ is the local spin-boson coupling strength. The Hamiltonian H_N commutes with the parity operator $\Pi = \exp\left[i\pi \sum_{n=1}^{N} (a_n^\dagger a_n + J_n^z + \frac{N_a}{2}) \right]$ and thus respects a global Z_2 symmetry in addition to the translational symmetry. However, the time reversal symmetry is broken due to the synthetic magnetic field. Note that we consider the limit of an infinite number of atoms in each cavity $N_a \to \infty$; thus, for any number of lattice sites N, the system realizes the thermodynamic limit of infinite particles. Below, we find a rich phase diagram as a function of $g = 2\lambda/\sqrt{\omega\Omega}$ and θ and anomalous critical properties as shown in Fig. 1 for $N = 3, 5$.

Anomalous normal phase with bounded fluctuation and correlation.— Let us begin by investigating the normal phase. In the thermodynamic limit, we introduce the Holstein-Primakoff transformation $J_n^+ \simeq \sqrt{N_a} b_n^\dagger$ and $J_n^z = N_a/2 - b_n^\dagger b_n$ with $\left[b_n, b_n^\dagger \right] = 1$ and perform a Fourier transform, $a_n^\dagger = \sum_k e^{ikn} a_k^\dagger / \sqrt{N}, b_n^\dagger = \sum_k e^{ikn} b_k^\dagger / \sqrt{N}$ with $k = 0, \pm 2\pi/N, \cdots, \pm(N-1)\pi/N$, to derive the effective Hamiltonian

$$H_{\rm np} = \sum_k \left[\omega_k a_k^\dagger a_k + \Omega b_k^\dagger b_k - \lambda (a_k + a_{-k}^\dagger)(b_{-k} + b_k^\dagger) \right], \tag{2}$$

where $\omega_k = \omega + 2J\cos(\theta - k)$. Note that only the modes with the same magnitude of momentum, $a_{\pm k}$ and $b_{\pm k}$, are coupled with each other; thus, the Hamiltonian can be diagonalized for each k. Four excitation energies are given by

$$\varepsilon_k^{(\pm)} = \sum_{j=1}^{2} \sqrt{A_{j,k}^{(\pm)}} + \Delta_k, \tag{3}$$

where $\Delta_k = (\omega_k - \omega_{-k})/4$. The superscripts $(\pm)$ denote the upper and lower branches of the excitation spectra, respectively, and the expressions of $A_{j,k}^{(\pm)}$ can be found in [48]. The upper branch is always gapped, $\varepsilon_k^{(+)} > 0$. For each momentum k, the lower branch excitation $\varepsilon_k^{(-)}$ can become zero. By

solving $\varepsilon_k^{(-)}=0$, we find $g_k(\theta)=\sqrt{2\omega_k\omega_{-k}/\omega(\omega_k+\omega_{-k})}$. At a given θ, the lowest value of g_k defines the critical point as $H_{\rm np}$ becomes unstable above this point, indicating the emergence of the superradiant phase. Namely, the critical point at θ is

$$g_c(\theta)=\min\{g_{k_j}(\theta)|k_j\}, \tag{4}$$

where $k_j=-2\pi j/N,\ j=0,1,\cdots,(N-1)/2$. We denote the momentum mode that realizes the minimum in Eq. 4 as k_c, the critical momentum. As the magnetic flux θ is varied, the critical momentum k_c also changes; thus, we define the flux critical points $\theta_c^{k_{j+1},k_j}$, which mark the boundary between the regions where the modes k_{j+1} and k_j become critical, respectively. These points are found by solving $g_{k_{j+1}}=g_{k_j}$ for θ. We find that $0<\theta_c^{k_{(N-1)/2},k_{(N-3)/2}}<\theta_c^{k_{(N-3)/2},k_{(N-5)/2}}<\cdots<\theta_c^{k_1,k_0}<\pi$. When $\theta>\theta_c^{k_1,k_0}$, the zero-momentum mode becomes critical, i.e., $k_c=k_0$, with a mean-field exponent of $1/2$. Interestingly, for $\theta<\theta_c^{k_1,k_0}$, a non-zero momentum mode becomes critical, i.e., $k_c\neq k_0$, with a non-mean-field exponent of 1 [see Fig. 1 (b) and (d)]. We refer to this as an anomalous NP, which spans $g<g_c(\theta<\theta_c^{k_1,k_0})$.

To understand the emergence of the anomalous NP, we note that ε_k from Eq. (3) consists of a sum of square root terms and a constant shift $\Delta_k=(\omega_k-\omega_{-k})/4=J\sin\theta\sin k$. The latter is the difference in frequencies of lattice photons with opposite momentums and it is non-zero only for $k\neq 0$ when the time-reversal symmetry is broken ($\theta\neq 0,\pi$). For $k_c=k_0$, $\Delta_{k_c=k_0}=0$; therefore, $\varepsilon^{(-)}_{k_c=k_0}$ closes the gap with the square root $\varepsilon^{(-)}_{k_c=k_0}\propto|g-g_c|^{1/2}$, a typical mean-field behavior. For $k_c\neq 0$, however, $\varepsilon^{(-)}_{k_c}$ becomes zero before the square root term becomes singular due to the cancelation with $\Delta_{k_c\neq k_0}<0$. In this case, the energy gap closes when an analytical function simply crosses the zero and the exponent becomes 1, i.e. $\varepsilon^{(-)}_{k_c\neq k_0}\propto|g-g_c|^1$. Furthermore, at the boundary between the normal phase and anomalous normal phase, namely, at $g_c(\theta_c^{k_1,k_0})$, we find that both the k_0 and k_1 mode simultaneously become critical, whose scaling exponents are $1/2$ and 1. In addition, at other flux critical points between the non-zero momentum modes, i.e., $\theta_c^{k_{i+1},k_i}$ with $i>0$, the two critical excitations with an identical exponent $\gamma=1$ appear [see Fig. 1(b)].

In the anomalous NP, the local photon number $\langle a^\dagger a\rangle_n$ and the bipartite entanglement $\mathcal{S}_n$ between the nth site and the rest of chain remains finite at the critical point [Fig. 2(a)]. This is a striking observation because the fluctuation and correlation are typically expected to diverge at the critical point [43, 46, 49]. To gain further insight, we adiabatically eliminate the atomic degrees of freedom in the infinitely frequency ratio limit ($\Omega/\omega\to\infty$) [31], and derive the analytical expression [48] for the excitation energy as $\varepsilon_k=\sqrt{A_k}+2\Delta_k$ and the photon number as

$$\langle a_n^\dagger a_n\rangle_{\rm np}=\frac{1}{N}\sum_k\left[\frac{\omega_k+\omega_{-k}}{2\sqrt{A_k}}-\frac{2\sqrt{A_k}}{\omega_k+\omega_{-k}}-2\right]. \tag{5}$$

From this, we see that $\langle a_n^\dagger a_n\rangle_{\rm np}\to\infty$ only if $\sqrt{A_k}\to 0$ and for the anomalous NP with $\Delta_k<0$, the photon number is bounded. This in turn leads to the bounded entanglement among cavity fields as the entanglement is generated by multimode squeezing with a bounded photon number. On the other hand, for $\theta>\theta_c^{k_1,k_0}$, both $\langle a^\dagger a\rangle_n$ and $\mathcal{S}_n$ diverges with mean-field exponent [48] as the photon number is proportional to the inverse of the square root term $\sqrt{A_k}$ in ε_k.

Multicriticality and frustration in the broken symmetry phase.— When $g>g_c(\theta)$, a second-order continuous phase transition occurs giving rise to spontaneous coherence i.e. $\langle a_n\rangle=x_n+iy_n\neq 0$. We first replace the operators in Eq. (1) with their mean values to derive the mean-field energy (see Supplementary Material [48] for the validity of the mean-field approximation). By minimizing the mean-field energy over the atomic degree of freedom [48], we have

$$\bar{E}_N=\sum_{n=1}^{N}\Big[\bar{x}_n^2+\bar{y}_n^2-\frac{1}{2}\sqrt{1+4g^2\bar{x}_n^2}+2\bar{J}\cos\theta(\bar{x}_n\bar{x}_{n+1}+\bar{y}_n\bar{y}_{n+1})+2\bar{J}\sin\theta(\bar{x}_{n+1}\bar{y}_n-\bar{x}_n\bar{y}_{n+1})\Big], \tag{6}$$

where $\bar{J}=J/\omega$, $\bar{E}=E/N_a\Omega$, $\bar{x}_n=\sqrt{\omega_0/N_a\Omega}\ x_n$, $\bar{y}_n=\sqrt{\omega_0/N_a\Omega}\ y_n$. We numerically minimize Eq. (6) and draw the phase diagram for $N=3$ and $N=5$ as shown in Figs. 1(a) and 1(c). For odd N, there exists $(N-1)/2$ first-order transition lines that meet with the continuous transition line $g_c(\theta)$ at each flux critical point $\theta_c^{k_i,k_{i+1}}$, making them tricritical points.

Here, we show that the origin of first-order transitions is the frustration of cavity fields, which leads to the recently discovered frustrated superradiant phase [40]. To this end, we derive an effective mean-field energy for the position quadrature x_n of the cavity fields only by eliminating the momentum quadrature y_n at the global minimum of Eq. (6) [48], which leads to

$$\bar{E}_N^{\rm GS}=\sum_{n=1}^{N}\left[\bar{x}_n^2-\frac{1}{2}\sqrt{1+4g^2\bar{x}_n^2}+\sum_{m=0}^{(N-1)/2}\bar{J}_m^{\rm eff}\bar{x}_n\bar{x}_{n+m}\right]. \tag{7}$$

Eq. (7) shows that the nearest-neighborhood complex photon hopping effectively realizes long-range interactions among $\bar{x}_n$ mediated by $\bar{y}_n$. In particular, we find that the dominant terms are the nearest and next-nearest neighborhood interaction, $|\bar{J}^{\rm eff}_{m>2}|\ll|\bar{J}^{\rm eff}_{1,2}|$. As the flux modulates signs and magnitudes of $\bar{J}_2^{\rm eff}$ and $\bar{J}_1^{\rm eff}$, frustrated sign configurations for $\bar{x}_n$ may occur, analogous to the J_1 and J_2 Ising model. We illustrate this point using N odd lattices.

For $N=3$, Eq. (7) becomes identical with the mean-field energy of the Dicke lattice model with a real photon hopping [40]. As shown in Fig. 1 (a), $\bar{J}_1^{\rm eff}$ changes the sign at the critical flux point $\theta=\theta_c^{k_1,k_0}$. Therefore, the broken symmetry phase undergoes a first-order phase transition between the non-frustrated SP for $\bar{J}_1^{\rm eff}<0$ and the frustrated SP for $\bar{J}_1^{\rm eff}>0$ with the ground-state degeneracy $D=6$. We note

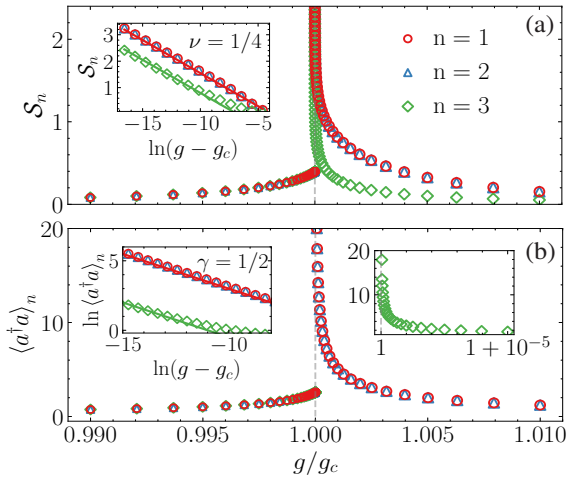


FIG. 2. (a) Bipartite entanglement between nth site with the two remaining sites and (b) photon number for nth cavity as a function of g/g_c for $N = 3$ and $\theta < \theta_c$ across the anomalous SPT. Lines are analytical and shapes are numerical results. Both quantities are bounded in the anomalous NP and divergent in the frustrated SP. The insets on the left side show scaling of the two quantities in the frustrated SP, both of which are $\gamma = 1/2$. In the right inset of (a) and (b), the divergence of the 3rd site is given separately as its peak is much narrower than the rest.

that a similar phase diagram has been found in the Rabi triangle model [41], which can also be understood from our effective description.

For $N = 5$, when $\theta < \theta_c^{k_2,k_1}$, one has $\bar{J}_1^{\text{eff}} > \bar{J}_2^{\text{eff}} > 0$ and the nearest neighbors should be anti-aligned to minimize the energy, which is incompatible with a 1D chain with odd N. Therefore, a frustrated configuration emerges where a single pair of neighboring sites are aligned, called a ferromagnetic pair, with $D = 10$. For $\theta > \theta_c^{k_2,k_1}$, one has $\bar{J}_2^{\text{eff}} > \bar{J}_1^{\text{eff}} > 0$ that favors the next-nearest neighbors x_n and x_{n+2} to be anti-aligned, which leads to a frustrated configuration with three ferromagnetic pair ($D = 10$). This configuration persists even when $\bar{J}_1^{\text{eff}}$ becomes negative; however, when the negative $\bar{J}_1^{\text{eff}}$ becomes the dominant energy scale and all x_n have the same sign, leading to a non-frustrated SP with the degeneracy $D = 2$. Our analysis can be straightforwardly extended to a larger lattice size for both odd and even N [48]. For even N, if $J_2 > 0$ is dominant over J_1, there could be frustration for odd $N/2$, but no frustration for even $N/2$.

Excitation and fluctuation in the superradiant phase.— Let us discuss the excitation and fluctuation in various SPs. For detailed derivation, we refer to Ref. [48]. For $\theta \geq \theta_c^{k_1,k_0}$, since all mean values $\bar{x}_n$ are identical with no frustration, the resulting effective Hamiltonian preserves the translational symmetry and we find that the k_0 momentum mode becomes critical, with the mean-field exponent $\gamma = 1/2$ [48]. For $0 < \theta < \theta_c^{k_1,k_0}$, the translational symmetry of the system is broken due to the frustration. Therefore, we numerically calculate the excitation spectra for $N = 3$, $N = 5$ [See Fig. 1(b)]. For $N = 3$, through asymptotic expansions, we analytically derive that the excitation energy gap closes with an exponent $3/2$ [48], which agrees with the numerical result. For $N = 5$, we find the exponent to be $5/2$. Therefore, we have

$$\begin{aligned} \varepsilon &\propto (g_c - g)^{\gamma_-} \qquad (\text{for } g < g_c) \\ \varepsilon &\propto (g - g_c)^{\gamma_+(N)} \qquad (\text{for } g > g_c) \end{aligned} \tag{8}$$

with $\gamma_- = 1$ and $\gamma_+(N) = N/2$ for $N = 3, 5$. We note that the possibility of having different critical exponents on both sides of phase transition has been recently discussed in Ref. [47] and the anomalous SPT in the synthetic magnetic fields exhibits such unique properties. This is qualitatively different from the scaling behavior of the previously reported frustrated SPT [40], where both sides of the transition share a mean-field exponent and an additional non-mean-field scaling appears in FSP. We also calculate the photon number and bipartite entanglement S_n in the SP. Unlike the anomalous NP where both are non-divergent, we find that they do diverge at the critical point as shown in Fig. 2 for $N = 3$. Therefore, there is a *discontinuity* of both quantities at the critical point of a continuous phase transition. We discovered that the SPT for $0 < \theta < \theta_c^{k_1,k_0}$ exhibits highly unusual anomalous critical properties summarized above, and hence we call it an anomalous SPT.

Anomalous multicritical points.— Finally, we discuss the properties at the multicritical points. We have found that there are two types of multicritical points: i) one is $g_c\left(\theta_c^{k_1,k_0}\right)$, where the boundary between the NP and anomalous NP and the boundary between non-frustrated and frustrated SP meet. At this point, two critical scalings for the closing energy gap with $\gamma = 1$ and $\gamma = 1/2$ coexist. ii) Others are $g_c\left(\theta_c^{k_{i+1},k_i}\right)$ with $1 \leq i \leq (N-3)/2$ where the momentum of the critical mode changes from k_i to k_{i+1} in the normal phase and the sign configuration for the frustrated SP changes. At this point, there are two critical modes on both sides of the multicritical point, but their exponents are both $\gamma = 1$. While it is generally expected that the critical exponents at the multicritical point are different from that of the continuous phase transition, two coexisting critical scalings are unique properties of multicritical points of the anomalous SPT.

Discussions.— The Dicke lattice model in the synthetic magnetic fields can be realized in various quantum systems that consist of coupled spins and bosons. The local spin-boson interactions can be implemented using ion-traps [50, 51], superconducting circuits [25, 26, 52], and cavity QED [53–55]. Moreover, the photon or phonon hopping can be engineered to form a desired lattice with a complex hopping energy [5, 56–61]. Our work demonstrates that the breaking of the time-reversal symmetry offers a unique mechanism for the normal phase of lattice bosons to become unstable with bounded fluctuation and that the complex nearest-neighborhood hopping amplitudes effectively mediate long-range interactions which may lead to exotic frustrated quantum phases of coupled light and matter. How the unique scaling properties of the anomalous SPT discovered here could be used for the applications

in critical metrology based on quantum optical models like Dicke/Rabi model is an interesting topic for future investigations [62–64].

Note added.— Upon completion of this work, we became aware of a recent work on the Rabi lattice models in synthetic magnetic fields [42].

Acknowledgments.— This work was supported by NSFC under Grant No. 12050410258, the Startup Fund and Summer Research Scholar Program from Duke Kunshan University, Kunshan Municipal Government research funding, and Innovation Program for Quantum Science and Technology 2021ZD0301602.

* myungjoong.hwang@duke.edu

[1] D. C. Tsui, H. L. Stormer, and A. C. Gossard, "Two-Dimensional Magnetotransport in the Extreme Quantum Limit," Phys. Rev. Lett. **48**, 1559–1562 (1982).
[2] R. B. Laughlin, "Anomalous Quantum Hall Effect: An Incompressible Quantum Fluid with Fractionally Charged Excitations," Phys. Rev. Lett. **50**, 1395–1398 (1983).
[3] R. O. Umucalılar and I. Carusotto, "Artificial gauge field for photons in coupled cavity arrays," Phys. Rev. A **84**, 043804 (2011).
[4] Nathan Schine, Albert Ryou, Andrey Gromov, Ariel Sommer, and Jonathan Simon, "Synthetic Landau levels for photons," Nature **534**, 671–675 (2016).
[5] P. Roushan, C. Neill, A. Megrant, Y. Chen, R. Babbush, R. Barends, B. Campbell, Z. Chen, B. Chiaro, A. Dunsworth, A. Fowler, E. Jeffrey, J. Kelly, E. Lucero, J. Mutus, P. J. J. O'Malley, M. Neeley, C. Quintana, D. Sank, A. Vainsencher, J. Wenner, T. White, E. Kapit, H. Neven, and J. Martinis, "Chiral ground-state currents of interacting photons in a synthetic magnetic field," Nature Phys **13**, 146–151 (2017).
[6] Charlie-Ray Mann, Simon A. R. Horsley, and Eros Mariani, "Tunable pseudo-magnetic fields for polaritons in strained metasurfaces," Nat. Photonics **14**, 669–674 (2020).
[7] Jens Koch, Andrew A Houck, Karyn Le Hur, and S M Girvin, "Time-reversal-symmetry breaking in circuit-QED-based photon lattices," Physical Review A **82**, 043811 – 18 (2010).
[8] Alejandro Bermudez, Tobias Schaetz, and Diego Porras, "Synthetic Gauge Fields for Vibrational Excitations of Trapped Ions," Phys. Rev. Lett. **107**, 150501 (2011).
[9] Hamed Abbaszadeh, Anton Souslov, Jayson Paulose, Henning Schomerus, and Vincenzo Vitelli, "Sonic Landau Levels and Synthetic Gauge Fields in Mechanical Metamaterials," Phys. Rev. Lett. **119**, 195502 (2017).
[10] Y.-J. Lin, R. L. Compton, K. Jiménez-García, J. V. Porto, and I. B. Spielman, "Synthetic magnetic fields for ultracold neutral atoms," Nature **462**, 628–632 (2009).
[11] N. R. Cooper, J. Dalibard, and I. B. Spielman, "Topological bands for ultracold atoms," Rev. Mod. Phys. **91**, 015005 (2019).
[12] Ling Lu, John D. Joannopoulos, and Marin Soljačić, "Topological photonics," Nature Photon **8**, 821–829 (2014).
[13] Alexander B. Khanikaev and Gennady Shvets, "Two-dimensional topological photonics," Nature Photon **11**, 763–773 (2017).
[14] Tomoki Ozawa, Hannah M. Price, Alberto Amo, Nathan Goldman, Mohammad Hafezi, Ling Lu, Mikael C. Rechtsman, David Schuster, Jonathan Simon, Oded Zilberberg, and Iacopo Carusotto, "Topological photonics," Rev. Mod. Phys. **91**, 015006 (2019).
[15] Daniele De Bernardis, Ze-Pei Cian, Iacopo Carusotto, Mohammad Hafezi, and Peter Rabl, "Light-Matter Interactions in Synthetic Magnetic Fields: Landau-Photon Polaritons," Phys. Rev. Lett. **126**, 103603 (2021).
[16] N.Y. Yao, C.R. Laumann, A.V. Gorshkov, H. Weimer, L. Jiang, J.I. Cirac, P. Zoller, and M.D. Lukin, "Topologically protected quantum state transfer in a chiral spin liquid," Nat Commun **4**, 1585 (2013).
[17] Alexander V. Poshakinskiy, Janet Zhong, Yongguan Ke, Nikita A. Olekhno, Chaohong Lee, Yuri S. Kivshar, and Alexander N. Poddubny, "Quantum Hall phases emerging from atom–photon interactions," npj Quantum Inf **7**, 34 (2021).
[18] Xin Wang, Tao Liu, Anton Frisk Kockum, Hong-Rong Li, and Franco Nori, "Tunable Chiral Bound States with Giant Atoms," Phys. Rev. Lett. **126**, 043602 (2021).
[19] John Clai Owens, Margaret G. Panetta, Brendan Saxberg, Gabrielle Roberts, Srivatsan Chakram, Ruichao Ma, Andrei Vrajitoarea, Jonathan Simon, and David I. Schuster, "Chiral cavity quantum electrodynamics," Nature Physics , 1–5 (2022).
[20] Klaus Hepp and Elliott H Lieb, "On the superradiant phase transition for molecules in a quantized radiation field: the dicke maser model," Annals of Physics **76**, 360–404 (1973).
[21] Y. K. Wang and F. T. Hioe, "Phase Transition in the Dicke Model of Superradiance," Phys. Rev. A **7**, 831–836 (1973).
[22] Clive Emary and Tobias Brandes, "Chaos and the quantum phase transition in the Dicke model," Phys. Rev. E **67**, 066203 (2003).
[23] Clive Emary and Tobias Brandes, "Quantum Chaos Triggered by Precursors of a Quantum Phase Transition: The Dicke Model," Phys. Rev. Lett. **90**, 044101 (2003).
[24] D. Nagy, G. Kónya, G. Szirmai, and P. Domokos, "Dicke-Model Phase Transition in the Quantum Motion of a Bose-Einstein Condensate in an Optical Cavity," Phys. Rev. Lett. **104**, 130401 (2010).
[25] Pierre Nataf and Cristiano Ciuti, "Vacuum Degeneracy of a Circuit QED System in the Ultrastrong Coupling Regime," Phys. Rev. Lett. **104**, 023601 (2010).
[26] Oliver Viehmann, Jan von Delft, and Florian Marquardt, "Superradiant Phase Transitions and the Standard Description of Circuit QED," Phys. Rev. Lett. **107**, 113602 (2011).
[27] Peter Kirton, Mor M. Roses, Jonathan Keeling, and Emanuele G. Dalla Torre, "Introduction to the Dicke Model: From Equilibrium to Nonequilibrium, and Vice Versa," Advanced Quantum Technologies **2**, 1800043 (2019).
[28] R. Botet, R. Jullien, and P. Pfeuty, "Size Scaling for Infinitely Coordinated Systems," Phys. Rev. Lett. **49**, 478–481 (1982).
[29] R. Botet and R. Jullien, "Large-size critical behavior of infinitely coordinated systems," Phys. Rev. B **28**, 3955–3967 (1983).
[30] Sébastien Dusuel and Julien Vidal, "Finite-Size Scaling Exponents of the Lipkin-Meshkov-Glick Model," Phys. Rev. Lett. **93**, 237204 (2004).
[31] Myung-Joong Hwang, Ricardo Puebla, and Martin B. Plenio, "Quantum Phase Transition and Universal Dynamics in the Rabi Model," Phys. Rev. Lett. **115**, 180404 (2015).
[32] Sarang Gopalakrishnan, Benjamin L. Lev, and Paul M. Goldbart, "Emergent crystallinity and frustration with Bose–Einstein condensates in multimode cavities," Nat. Phys **5**, 845–850 (2009).
[33] Philipp Strack and Subir Sachdev, "Dicke Quantum Spin Glass of Atoms and Photons," Phys. Rev. Lett. **107**, 277202 (2011).
[34] Sarang Gopalakrishnan, Benjamin L. Lev, and Paul M. Gold-

bart, "Frustration and Glassiness in Spin Models with Cavity-Mediated Interactions," Phys. Rev. Lett. **107**, 277201 (2011).
[35] Sarang Gopalakrishnan, Benjamin L. Lev, and Paul M. Goldbart, "Exploring models of associative memory via cavity quantum electrodynamics," Philos. Mag. **92**, 353–361 (2012).
[36] Michael Buchhold, Philipp Strack, Subir Sachdev, and Sebastian Diehl, "Dicke-model quantum spin and photon glass in optical cavities: Nonequilibrium theory and experimental signatures," Phys. Rev. A **87**, 063622 (2013).
[37] Brendan P. Marsh, Yudan Guo, Ronen M. Kroeze, Sarang Gopalakrishnan, Surya Ganguli, Jonathan Keeling, and Benjamin L. Lev, "Enhancing Associative Memory Recall and Storage Capacity Using Confocal Cavity QED," Phys. Rev. X **11**, 021048 (2021).
[38] Alessio Chiocchetta, Dominik Kiese, Carl Philipp Zelle, Francesco Piazza, and Sebastian Diehl, "Cavity-induced quantum spin liquids," Nat. Commun. **12**, 5901 (2021).
[39] Shane P. Kelly, Ana Maria Rey, and Jamir Marino, "Effect of Active Photons on Dynamical Frustration in Cavity QED," Phys. Rev. Lett. **126**, 133603 (2021).
[40] Jinchen Zhao and Myung-Joong Hwang, "Frustrated Superradiant Phase Transition," Phys. Rev. Lett. **128**, 163601 (2022).
[41] Yu-Yu Zhang, Zi-Xiang Hu, Libin Fu, Hong-Gang Luo, Han Pu, and Xue-Feng Zhang, "Quantum Phases in a Quantum Rabi Triangle," Phys. Rev. Lett. **127**, 063602 (2021).
[42] Diego Fallas Padilla, Han Pu, Guo-Jing Cheng, and Yu-Yu Zhang, "Understanding the Quantum Rabi Ring Using Analogies to Quantum Magnetism," Phys. Rev. Lett. **129**, 183602 (2022).
[43] Neill Lambert, Clive Emary, and Tobias Brandes, "Entanglement and the Phase Transition in Single-Mode Superradiance," Physical Review Letters **92**, 073602 (2003).
[44] John L. Cardy, *Scaling and renormalization in statistical physics*, Cambridge lecture notes in physics No. 5 (Cambridge University Press, 1996).
[45] Mehran Kardar, *Statistical physics of fields* (Cambridge University Press, 2007).
[46] Subir Sachdev, *Quantum Phase Transitions*, 2nd ed. (Cambridge University Press, 2011).
[47] F. Léonard and B. Delamotte, "Critical Exponents Can Be Different on the Two Sides of a Transition: A Generic Mechanism," Phys. Rev. Lett. **115**, 200601 (2015).
[48] See Supplemental Material at [URL will be inserted by publisher] for further explanation and details of the calculation.
[49] A. Osterloh, Luigi Amico, G. Falci, and Rosario Fazio, "Scaling of entanglement close to a quantum phase transition," Nature **416**, 608–610 (2002).
[50] A. Safavi-Naini, R. J. Lewis-Swan, J. G. Bohnet, M. Gärttner, K. A. Gilmore, J. E. Jordan, J. Cohn, J. K. Freericks, A. M. Rey, and J. J. Bollinger, "Verification of a many-ion simulator of the dicke model through slow quenches across a phase transition," Phys. Rev. Lett. **121**, 040503 (2018).
[51] J Cohn, A Safavi-Naini, R J Lewis-Swan, J G Bohnet, M Gärttner, K A Gilmore, J E Jordan, A M Rey, J J Bollinger, and J K Freericks, "Bang-bang shortcut to adiabaticity in the Dicke model as realized in a Penning trap experiment," New J. Phys. **20**, 055013 (2018).
[52] L. J. Zou, D. Marcos, S. Diehl, S. Putz, J. Schmiedmayer, J. Majer, and P. Rabl, "Implementation of the dicke lattice model in hybrid quantum system arrays," Phys. Rev. Lett. **113**, 023603 (2014).
[53] Kristian Baumann, Christine Guerlin, Ferdinand Brennecke, and Tilman Esslinger, "Dicke quantum phase transition with a superfluid gas in an optical cavity," Nature **464**, 1301–1306 (2010).
[54] Ronen M. Kroeze, Yudan Guo, Varun D. Vaidya, Jonathan Keeling, and Benjamin L. Lev, "Spinor Self-Ordering of a Quantum Gas in a Cavity," Phys. Rev. Lett. **121**, 163601 (2018).
[55] Jens Klinder, Hans Keßler, Matthias Wolke, Ludwig Mathey, and Andreas Hemmerich, "Dynamical phase transition in the open Dicke model," Proc Natl Acad Sci USA **112**, 3290–3295 (2015).
[56] Yi Yang, Chao Peng, Di Zhu, Hrvoje Buljan, John D. Joannopoulos, Bo Zhen, and Marin Soljačić, "Synthesis and observation of non-Abelian gauge fields in real space," Science **365**, 1021–1025 (2019).
[57] John P. Mathew, Javier del Pino, and Ewold Verhagen, "Synthetic gauge fields for phonon transport in a nano-optomechanical system," Nat. Nanotechnol. **15**, 198–202 (2020).
[58] Yuan Chen, Yan-Lei Zhang, Zhen Shen, Chang-Ling Zou, Guang-Can Guo, and Chun-Hua Dong, "Synthetic Gauge Fields in a Single Optomechanical Resonator," Phys. Rev. Lett. **126**, 123603 (2021).
[59] Yuqing Li, Jiahui Zhang, Yunfei Wang, Huiying Du, Jizhou Wu, Wenliang Liu, Feng Mei, Jie Ma, Liantuan Xiao, and Suotang Jia, "Atom-optically synthetic gauge fields for a noninteracting Bose gas," Light Sci Appl **11**, 13 (2022).
[60] Javier del Pino, Jesse J. Slim, and Ewold Verhagen, "Non-Hermitian chiral phononics through optomechanically induced squeezing," Nature **606**, 82–87 (2022).
[61] Anika Frölian, Craig S. Chisholm, Elettra Neri, Cesar R. Cabrera, Ramón Ramos, Alessio Celi, and Leticia Tarruell, "Realizing a 1D topological gauge theory in an optically dressed BEC," Nature **608**, 293–297 (2022).
[62] Louis Garbe, Matteo Bina, Arne Keller, Matteo G. A. Paris, and Simone Felicetti, "Critical quantum metrology with a finite-component quantum phase transition," Phys. Rev. Lett. **124**, 120504 (2020).
[63] Yaoming Chu, Shaoliang Zhang, Baiyi Yu, and Jianming Cai, "Dynamic Framework for Criticality-Enhanced Quantum Sensing," Phys. Rev. Lett. **126**, 010502 (2021).
[64] Theodoros Ilias, Dayou Yang, Susana F. Huelga, and Martin B. Plenio, "Criticality-Enhanced Quantum Sensing via Continuous Measurement," PRX Quantum **3**, 010354 (2022).